Journal of Cerebral Blood Flow & Metabolism (2010) 30, 1384–1393

www.jcbfm.com

Blood–brain barrier permeability for ammonia in patients with different grades of liver fibrosis is not different from healthy controls

Annemarie Goldbecker[1,6], Ralph Buchert[2,6], Georg Berding[3], Martin Bokemeyer[4], Ralf Lichtinghagen[5], Florian Wilke[2], Björn Ahl[1] and Karin Weissenborn[1]

[1]*Department of Neurology and Clinical Neurophysiology, Hannover Medical School, Hannover, Germany;* [2]*Department of Nuclear Medicine, University Hospital Hamburg-Eppendorf, Hamburg, Germany;* [3]*Department of Nuclear Medicine, Hannover Medical School, Hannover, Germany;* [4]*Institute for Diagnostic and Interventional Neuroradiology, Hannover Medical School, Hannover, Germany;* [5]*Institute for Clinical Chemistry, Hannover Medical School, Hannover, Germany*

Increased blood-brain barrier (BBB) permeability for ammonia is considered to be an integral part of the pathophysiology of hepatic encephalopathy (HE) in patients with liver cirrhosis. Increased glutamate-/glutamine-signal intensity in magnetic resonance spectroscopic studies of the brain in cirrhotic patients was explained as a consequence of increased cerebral ammonia uptake. As similar spectroscopic alterations are present in patients with liver fibrosis, we hypothesized that BBB permeability for ammonia is already increased in liver fibrosis, and thereby contributing to the development of HE. To test this hypothesis, cerebral perfusion and ammonia metabolism were examined through positron emission tomography with ^{15}O-water, respectively, ^{13}N-ammonia in patients with Ishak grades 2 and 4 fibrosis, cirrhosis, and healthy controls. There were neither global nor regional differences of cerebral blood flow, the rate constant of unidirectional transport of ammonia from blood into brain tissue, the permeability surface area product of the BBB for ammonia, the net metabolic clearance rate constant of ammonia from blood into glutamine in brain, or the metabolic rate of ammonia. The hypothesis that increased permeability of the BBB for ammonia in patients with liver fibrosis contributes to the later development of HE could not be supported by this study.
Journal of Cerebral Blood Flow & Metabolism (2010) **30,** 1384–1393; doi:10.1038/jcbfm.2010.22; published online 10 March 2010

Keywords: cerebral ammonia metabolism; cerebral blood flow; hepatic encephalopathy; matrix metalloproteinases; positron emission tomography

Introduction

Ammonia is regarded to have a major role in the disturbance of neurotransmission, cellular energy metabolism, and cell swelling in hepatic encephalopathy (HE) (Butterworth, 2003). In the blood, ammonia exists in gaseous (NH_3) and ionic (NH_4^+) form. The electric charge of the ammonium ion prevents its passage across the blood–brain barrier (BBB), so that ammonia gets access to the brain through diffusion of the gaseous form, the fraction of which however is rather small at physiological pH levels (Lockwood *et al*, 1980). In the brain, ammonia is metabolized into glutamine by binding to glutamate through the glutamine synthetase (Figure 1). Cerebral ammonia metabolism has been studied predominantly in rats, monkeys, and healthy human subjects (Cooper *et al*, 1979; Lockwood *et al*, 1980, 1984; Phelps *et al*, 1977; Keiding *et al*, 2006). Only three studies in patients with liver cirrhosis exist (Ahl *et al*, 2004; Keiding *et al*, 2006; Lockwood *et al*, 1991). All used positron emission tomography (PET) for analysis of the cerebral ammonia metabolism, two included a control group. Lockwood *et al* (1991) found a significantly increased BBB permeability for ammonia in patients with minimal HE compared with controls. Ahl *et al* (2004) showed a trend to a lower initial uptake rate K_1 and BBB permeability for

Correspondence: Dr A Goldbecker, Department of Neurology and Clinical Neurophysiology, Hannover Medical School, Hannover 30623, Germany.
E-mail: goldbecker.annemarie@mh-hannover.de
[6]These authors contributed equally to the work.
Received 21 July 2009; revised 31 January 2010; accepted 1 February 2010; published online 10 March 2010

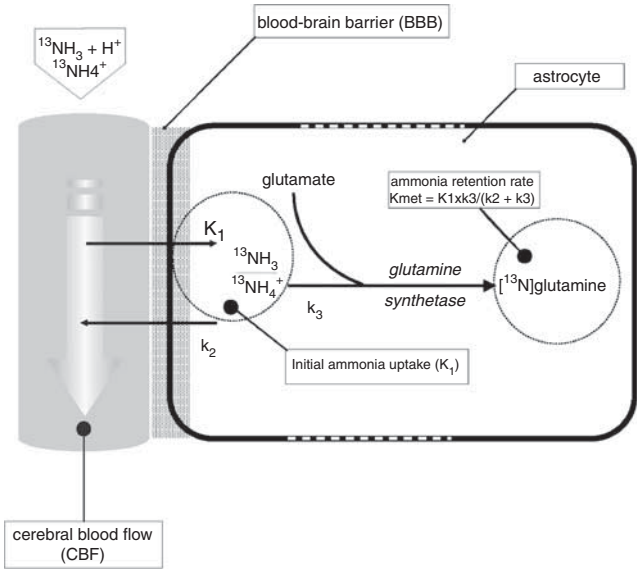

Figure 1 Model of cerebral ammonia metabolism.

ammonia in patients with minimal and grade 1 HE compared with cirrhotic patients without HE, with all values being higher than Lockwood's control data. Keiding *et al* (2006) found no differences in the ammonia BBB permeability and K_1 between cirrhotic patients with and without HE and healthy controls. Their study had not been published when this study started. Considering the data of Lockwood *et al* (1991) and Ahl *et al* (2004), we hypothesized that alteration of BBB permeability for ammonia starts early in the course of liver disease, i.e., in liver fibrosis. The observation of elevated glutamate-/glutamine levels in magnetic resonance spectroscopy (MRS) performed in the brain of patients with chronic hepatitis and liver fibrosis but no cirrhosis compared with controls (own unpublished data) was a further back up for this hypothesis.

To test the hypothesis, cerebral ammonia metabolism was studied in patients with Ishak score F2 and F4 fibrosis compared with patients with cirrhosis (F6) and healthy controls.

Patients and methods

Six healthy controls (three female, 55 ± 7 years) and 18 patients (nine female, 55 ± 10 years), subdivided into three patient groups according to the Ishak fibrosis score, were prospectively included into this study. Liver fibrosis F2 ($n = 6$) and F4 ($n = 6$) was proven by biopsy. Liver cirrhosis (F6; $n = 6$) was proven by biopsy in five patients and by ultrasound in one patient. All patients suffered from chronic viral hepatitis (hepatitis C $n = 17$, hepatitis B $n = 1$) and were classified CHILD A (Pugh *et al*, 1973). No patient had clinical signs of HE. Two patients of the F4- and two of the cirrhosis group achieved a pathological portosystemic encephalopathy (PSE)-Syndrom-Test result (score < -4) (Schomerus *et al*, 1999). Patients and controls underwent magnetic resonance imaging (MRI), ^{15}O-water-, and ^{13}N-ammonia-PET. In addition, tumor necrosis factor-α (TNF-α); transforming growth factor-β1 (TGF-β1); the matrix metalloproteinases MMP1, 2, and 9; and the tissue inhibitors of MMPs TIMP1 and 2 were assessed in the blood as alterations of the BBB in patients with liver fibrosis could be because of the activation of these proteases during inflammatory processes in the liver. PET data of three patients of the cirrhosis group could not be evaluated because of technical problems. Among these were those two cirrhosis patients with a pathological PSE-Syndrom-Test result. Thus, there were only three patients left in the cirrhosis group. Therefore, the data of the cirrhosis group are presented, but they were not included in the statistical analyses (analysis of variance, ANOVA).

The study had been approved by the local ethics committee and the Federal Office for Radiation Protection. All patients and controls gave their written informed consent. The study protocol conformed to the ethical guidelines of the 1975 (revised in 1983) Declaration of Helsinki.

Positron Emmission Tomography

An ECAT EXACT 922/47 full-ring whole-body tomograph was used for PET imaging (Siemens, Erlangen, Germany).

^{15}O-water-PET was performed as a 5 mins dynamic acquisition of 20 frames (12×5, 4×15, 2×30, and 2×60 secs) starting with intravenous bolus injection of about 3.7 GBq ^{15}O-water. The input function was obtained by fully automated blood sampling of arterial blood.

After an interval of 40 mins, ^{13}N-ammonia-PET was performed as a 23.5 mins dynamic acquisition of 20 frames (12×10, 5×30, 2×120, and 1×900 secs) starting with intravenous injection of about 740 MBq ^{13}N-ammonia. Arterial blood samples were taken manually at mid-frame times and measured in a well counter cross-calibrated with the PET system.

For attenuation correction, a transmission scan with rotating ^{68}Ge/^{68}Ga sources was acquired for 10 mins before each scan. All scans were acquired in 2D mode. Transaxial images were obtained by iterative reconstruction. Spatial resolution in the reconstructed images was about 7 mm full-width-at-half-maximum.

Magnetic Resonance Imgaging

Conventional MRI (1.5 T, Signa Horizon, GE Medical Systems, Milwaukee, WI, USA) was performed to exclude cerebral lesions and for use in stereotactical normalization of the PET images.

Biochemical Analysis

Heparinized plasma was collected for measurement of TNF-α, TGF-β1, TIMP1, and MMP9 and serum for MMP1, TIMP2, and MMP2 measurement (Human Biotrak Easy ELISA; GE Healthcare, Amersham Biosciences, Buckinghamshire, UK). In addition, arterial plasma ammonia, bilirubin, albumin, cholin esterase, and arterial gases

including pH were determined. Blood gas analysis was performed immediately after sample collection.

Tracer Kinetic Modeling

First, the 'Realign' tool of the Statistical Parametric Mapping software package (SPM2, Welcome Department of Cognitive Neurology, University College, London, UK) was used to correct each individual dynamic PET sequence for eventual head motion during the acquisition. The last frame served as reference for realignment. As frames 1 to 4 (first 20 secs) of the ^{15}O-water-PET did not provide sufficient anatomical information for convergence of the realign algorithm in most subjects, the transformation matrix for realignment of frame 5 was applied to these early frames, assuming that there was no relevant motion during this time. In case of ^{13}N-ammonia, the first six frames (first minute) did not provide sufficient anatomical information, and, therefore, were treated analogously. The difference of the anatomical information content in the early frames between ^{15}O-water- and ^{13}N-ammonia-PET was not only because of differences in tracer kinetics, but also because of different injection techniques. ^{15}O-water was injected as a short bolus of about 7 secs by an automatic injector, whereas ^{13}N-ammonia was injected manually as a slow bolus (maximum 30 secs). The translation required for realignment was smaller than 6 mm in all scans except two. There was movement of about 10 mm in the ^{15}O-water scan of a control subject, and of about 13 mm in the ^{13}N-ammonia scan in an F2 subject. The movement was primarily in horizontal–transversal direction (*x* direction) in both cases. Exclusion of these two subjects did not significantly affect the results of this study.

To support standardized identification of volumes of interest (VOIs), each motion-corrected sequence was stereotactically normalized as follows: (i) a representative static PET uptake image obtained by integrating all frames of the dynamic sequence (each frame weighted by its duration) was coregistered to the individual MRI using the 'Coregister' tool of SPM2, (ii) the individual MRI was stereotactically normalized to the T1 template of SPM2 using SPM2's 'Normalize' tool (default parameter settings), and (iii) the dynamic PET sequence was stereotactically normalized by applying the transformation of the MRI normalization to each of its frames.

Fifteen VOIs were examined, predefined in template space by the automated anatomic labeling atlas made available by Tzourio-Mazoyer *et al* (2002): caudate nucleus, anterior, middle and posterior cingulate, lentiforme nucleus, pons, supplementary motor area, thalamus, cerebellum, frontal, motor, occipital, parietal and temporal cortex, and white matter. A 'whole brain' VOI for assessment of 'global' parameters was obtained by the union of these VOIs (Figure 2).

Time activity curves (TACs) of ^{15}O-water and ^{13}N-ammonia were obtained for each subject and each VOI by averaging tracer concentration in the stereotactically

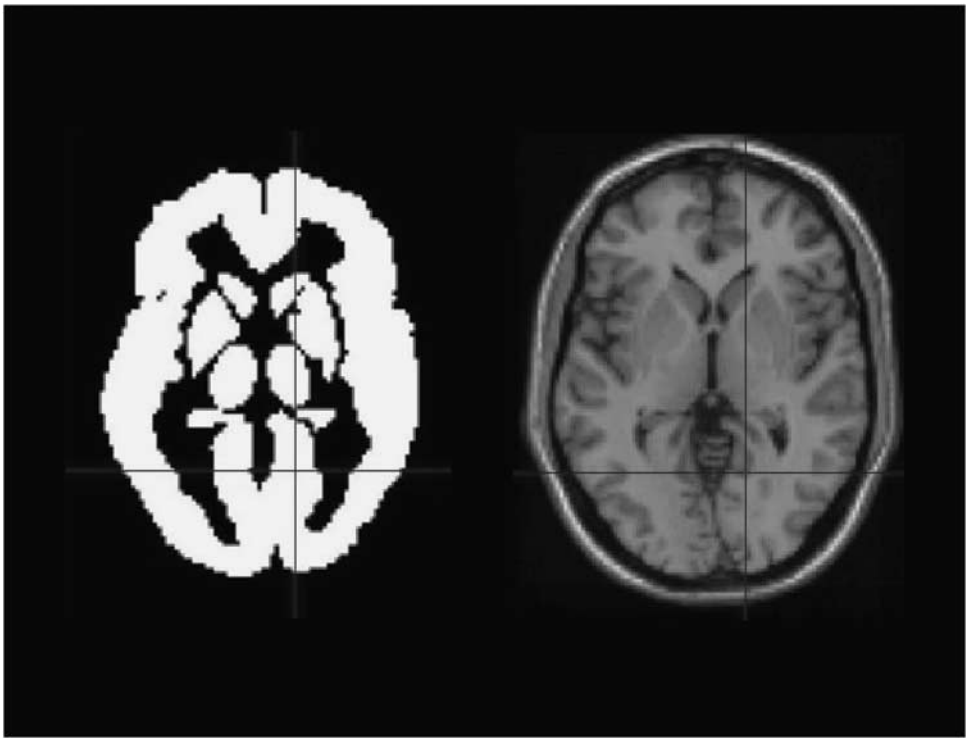

Figure 2 Whole brain VOI for assessment of 'global' parameters obtained by the union of the 15 standard VOIs (see text) predefined in template space by the automated anatomic labeling (AAL) atlas made available by Tzourio-Mazoyer *et al* (2002). Shown is a transversal slice of the whole brain VOI (left) and the corresponding slice of the single subject T1 template of SPM2 (right), with corresponding cross-hairs.

normalized sequences over all voxel values within the given VOI. Tracer kinetic modeling of the VOI-based TACs was performed using the kinetic tool of the PMOD software package (version 2.65, PMOD Technologies Ltd, Adliswil, Switzerland).

^{15}O-water TACs were analyzed using PMOD's 'Flow & Dispersion' model, which allows simultaneous fitting of the fractional arterial blood volume (fbv), cerebral blood flow (CBF), the tissue blood partition coefficient p, as well as delay Δt and dispersion τ of the measured arterial input function relative to true influx in the brain (Carroll *et al*, 2002). Delay and dispersion of the input function were obtained once for each subject by application of the full model to the whole brain TAC (start values of the fit $fbv = 0.02$, $CBF = 0.6$ mL blood/mL tissue/min, $CBF/p = 0.7$/min, $\Delta t = 0$ secs, $\tau = 0$ secs). The quality of the fit was checked by visual inspection of the residuals (Figure 3). Sensitivity analysis revealed that fbv and dispersion could not be separated, as was to be expected, because the two corrections have similar structure. However, this issue of identification did not affect the estimate of CBF, which could be identified reliably. Neither dispersion nor fbv results were used in the analyses of this study. For all other VOIs, delay and dispersion were fixed at the values obtained in the whole brain TAC in the same subject (start values of the other parameters as specified above).

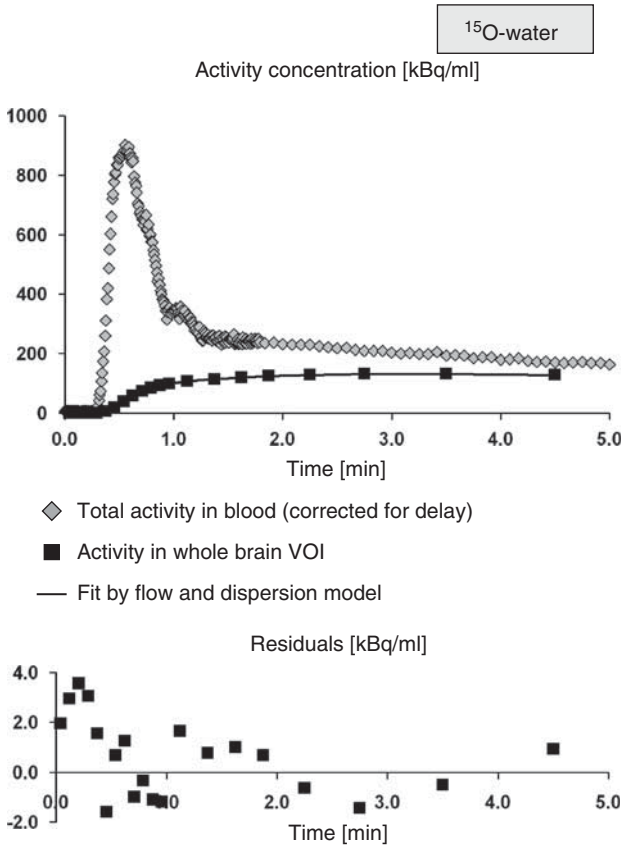

Figure 3 ^{15}O-water TACs in one representative subject (Ishak score 2). The upper part of the figure shows the delay corrected ^{15}O-water activity in blood (input function), the TAC in the whole brain VOI, and the fit by the flow and dispersion model. The lower part of the figure shows the residuals of the fit (note the different scaling of the y axis, the residuals are of the order of 1%). The perfusion was estimated to 0.291 mL/mL/min (coefficient of variance 2.5%). ^{13}N-ammonia TACs of this subject are shown in Figure 4.

^{13}N-ammonia TACs were first analyzed using the irreversible ($k_4 = 0$) (Innis *et al*, 2007) two-tissue compartment model for a simultaneous fit of the fbv, the rate K_1 of unidirectional transport of ^{13}N-ammonia from arterial blood into tissue, the clearance rate k_2 of ^{13}N-ammonia from tissue, and the conversion k_3 of ^{13}N-ammonia in tissue to ^{13}N-glutamine, as well as the delay Δt of the input function. Again, the delay of the input function was determined once from the whole brain TAC and then fixed at this value for all other TACs of the same subject (start values of the other parameters: $fbv = 0.04$, $K_1 = 0.2$ mL blood/mL tissue/min, $k_2 = 0.02$/min, $k_3 = 0.2$/min). The analysis included the whole dynamic scan corresponding to the time interval 0 to 23.5 mins. To obtain the ^{13}N-ammonia input function from the measured total activity in blood, metabolite correction was performed according to the data by Rosenspire *et al* (1990) who reported the fraction of unmetabolized ^{13}N-ammonia at 1, 2, 3, 4, and 5 mins after intravenous injection of ^{13}N-ammonia to be $93.1\% \pm 4.9\%$, $94.0\% \pm 2.8\%$, $81.8\% \pm 10.5\%$, $74.7\% \pm 13.4\%$, and $50.2\% \pm 18.9\%$, respectively. These data were inter- and extrapolated by the model

$$\text{parent fraction}\,(\%) = \begin{cases} 100 & t < t_0 \\ 100 * \exp(-\ln(2) * (t - t_0)/T_{1/2}) & t \geq t_0 \end{cases}$$

with $t_0 = 0.48$ mins and $T_{1/2} = 6.69$ mins. The same model was used by Ahl *et al* (Ahl *et al*, 2004; van den Hoff *et al*, 2001). Brain uptake of radioactive metabolites was neglected. The (uncorrected) time curve of total activity in blood was used for modeling of fbv. The Levenberg–Marquardt option and uniform weights were used for nonlinear regression. The quality of the fit was checked by visual inspection of the residuals (Figure 4A).

Dispersion was not included in the ammonia model, because the two-tissue compartment model implemented in the PMOD software package does not offer modeling dispersion of the input function, but its delay only. This is justified by the fact that the errors for the rate constants by neglecting dispersion are very small under reasonable experimental conditions if the delay is adjusted freely (van den Hoff *et al*, 1993). Therefore, it appears adequate in the tracer kinetic modeling to account for delay only, if only the rate constants are to be determined and the actual value of the delay is of no interest.

Permeability surface (PS_{BBB}) was calculated according to the formula $PS_{BBB} = -CBF \ln(1 - K_1/CBF)$.

The full kinetic modeling within the irreversible two-tissue compartment model did not allow reliable estimates of k_3 nor of the net metabolic clearance K_{met} ($= K_1^* k_3/(k_2 + k_3)$) of ^{13}N-ammonia from arterial blood into glutamine in brain tissue, which is required to compute the cerebral metabolic rate of ammonia (CMRA, see below). Therefore, Gjedde–Patlak plot analysis (Gjedde, 1982; Patlak *et al*, 1983) of the ^{13}N-ammonia TACs was performed to estimate K_{met} (Figure 4B). The metabolite-corrected input function

was used. The start time of the linear fit was variable, i.e., it was optimized individually in each fit.

CMRA was obtained by multiplying K_{met} with the arterial plasma ammonia concentration [A], i.e., $CMRA = K_{met}$ [A].

Statistical Analysis

Univariate ANOVA was used to compare CBF, K_1, PS_{BBB}, K_{met}, and CMRA between the two fibrosis groups (F2, F4) and the controls. The cirrhosis group was not included in the ANOVA (see Patients and methods). Scheffe's or Tamhane's *post hoc* test was applied in case of a significant ANOVA effect, dependent on the result of Levene's test of homogeneity of variances. The analysis was performed separately for each VOI. Bonferroni adjustment for the number of VOIs was not applied. Blood parameters were correlated with PET parameters using Spearman's non-parametric rank correlation test within the entire sample of subjects, i.e., all patients and all controls were included in the correlation analyses ($n = 21$). An effect was considered statistically significant if the two-sided significance level $\alpha \leqslant 0.05$ was reached.

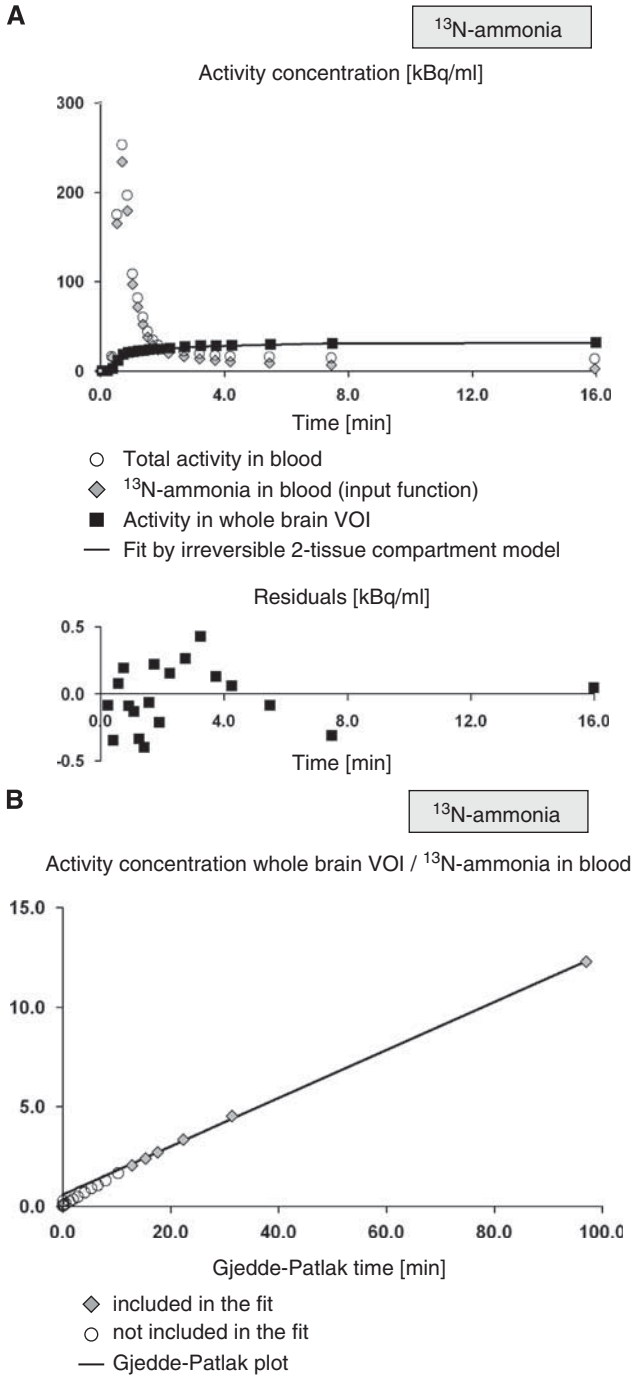

Results

Positron Emmission Tomography

TACs of ^{15}O-water and ^{13}N-ammonia of a representative subject, and their fits by the modeling are shown in Figures 3 and 4, respectively. Global CBF, K_1, PS_{BBB}, K_{met}, and CMRA are summarized in Table 1. ANOVA did not reveal a statistically significant difference between F2, F4 and controls with respect to any of these global parameters (Table 1). The differences in the ratio K_{met}/K_1 and in the intercept of the Gjedde–Patlak plot also did not reach the level of statistical significance (Table 1). ANOVA of regional CBF, K_1, and PS_{BBB} did not reveal any significant effect, too.

Biochemical Results

Ammonia concentration in plasma did not differ between the two fibrosis groups (F2, F4) and the controls (ANOVA: $P = 0.465$, Table 1). Neither did pH ($P = 0.449$), bilirubin ($P = 0.569$), and albumin ($P = 0.052$). Cholin esterase differed between the groups (controls: 9.76 ± 2.07 kU/L, F2: 7.69 ± 1.42 kU/L, F4: 6.57 ± 1.50 kU/L, ANOVA: $P = 0.016$). *Post hoc* testing revealed the reduction in the F4 group compared with the controls to be significant (Scheffe: $P = 0.018$), but the value was still within the normal range (5.32 to 11.25 kU/L).

Figure 4 ^{13}N-ammonia TACs in one representative subject (Ishak score 2, the same subject as in Figure 3). In (**A**), the time curve of total activity in blood (used for estimation of fbv), the time curve of ^{13}N-ammonia in blood (input function) obtained by population-based metabolite correction from the total blood activity, the TAC in the whole brain VOI, the fit by the irreversible two-tissue compartment model, and the residuals of the fit were shown. Model estimates in this case were delay = 3.3 secs (coefficient of variance 12.9%), *fbv* = 3.6% (3.5%), $K_1 = 0.158$ mL/mL/min (0.6%). In (**B**), the corresponding Gjedde–Patlak plot that resulted in slope = $K_{met} = 0.115$ mL/mL/min (2.2%) and intercept = 0.565 mL/mL (19.5%) is shown. The ratio K_{met}/K_1 was 0.73, and the permeability surface area product PS_{BBB} for ammonia was computed to 0.228 mL/mL/min.

Table 1 Global values (whole brain VOI)

	$P\text{-}NH_3$ (μmoL/L)	CBF (mL/mL/min)	K_1 (mL/mL/min)	PS_{BBB} (mL/mL/min)	K_{met} (mL/mL/min)	CMRA (nmol/mL/min)	K_{met}/K_1	Intercept Gjedde–Patlak plot (mL/mL)
Controls ($n=6$)	20.7 ± 2.3	0.330 ± 0.038	0.155 ± 0.026	0.213 ± 0.046	0.091 ± 0.025	1.886 ± 0.543	0.578 ± 0.134	0.577 ± 0.121
F2 ($n=6$)	22.8 ± 8.1	0.324 ± 0.059	0.156 ± 0.016	0.215 ± 0.030	0.113 ± 0.011	2.522 ± 0.735	0.731 ± 0.068	0.724 ± 0.122
F4 ($n=6$)	25.5 ± 7.7	0.289 ± 0.045	0.166 ± 0.016	0.257 ± 0.059	0.109 ± 0.017	2.807 ± 1.103	0.658 ± 0.110	0.599 ± 0.111
ANOVA (controls, F2, F4): *P*-value	0.465	0.319	0.597	0.217	0.130	0.177	0.101	0.098
F6 ($n=3$)	30.3 ± 13.4	0.347 ± 0.088	0.166 ± 0.027	0.226 ± 0.029	0.122 ± 0.012	3.805 ± 1.901	0.756 ± 0.180	0.723 ± 0.197

TNF-α was below the detection limit in all but one case (patient with F4 fibrosis). MMP1 ($P=0.260$), TIMP2 ($P=0.534$), TIMP1 ($P=0.111$), and MMP 9 ($P=0.105$) did not differ significantly between the two fibrosis groups (F2, F4) and the controls. MMP2 was significantly higher in patients with F2 fibrosis (2,776 ± 355 ng/mL) than in controls (2,083 ± 300 ng/mL) (ANOVA: $P=0.022$; Scheffe: $P=0.043$). It was also higher in the F4 group (2,747 ± 580 ng/mL), although this difference did not fully reach the level of statistical significance ($P=0.053$). Bivariate Spearman analysis for correlation of any of the global PET parameters (CBF, K_1, PS_{BBB}, K_{met}, CMRA) with MMP2 revealed no effect.

Discussion

The 1991 study of Lockwood *et al* (1991) was considered a milestone in the clarification of the pathophysiology of HE. Their suggestion of an increased permeability of the BBB for ammonia in patients with liver cirrhosis and HE gave direction to the interpretation of clinical and experimental data, and was also the basis to focus therapeutic endeavors on plasma ammonia-lowering strategies. The observation of a lower—though not statistically different—PS product of ammonia in cirrhotic patients with HE compared with patients without HE (Ahl *et al*, 2004) gave reason to hypothesize that the BBB permeability for ammonia decreases with increasing grade of HE. In consequence, it was discussed which way the PS product would behave in lower grades of chronic liver disease. The metabolic correlate of cerebral ammonia metabolism is the cerebral glutamine content represented by the glutamate-/glutamine peak in MRS. Interestingly, increased glutamate-/glutamine/creatin levels have been observed even in patients with compensated cirrhosis without any signs of HE (Köstler, 1998), and a personal observation in patients with chronic hepatitis showed increased concentrations compared with controls even in the absence of cirrhosis. When we observed, finally, that brain function in cirrhotic patients related to the extent of MRS changes but not to the extent of the actual ammonia uptake and metabolism rate (Weissenborn *et al*, 2007), we hypothesized that a patient's individual sensitivity against an actual ammonia load differs depending on former cerebral ammonia burden (which might be reflected in the metabolite levels measured by MRS), and that cerebral ammonia load may be increased even in patients with liver fibrosis because of cytokine-induced alterations of the BBB whereas it decreases again with progression of liver disease and HE. This study aimed to assess this hypothesis.

Actually, the hypothesis of an increased BBB permeability for ammonia in patients with liver fibrosis could not be confirmed. Neither CMRA nor PS_{BBB} differed significantly between the groups.

Blood levels of TNF-α; MMP1, 2, and 9; TIMP1 and 2; and TGF-β1 have been assessed to be correlated with the parameters representing BBB permeability for ammonia. It was hypothesized that the grade of inflammation in the liver represented by these parameters might relate to alterations of the BBB permeability. MMP2 was the only protease to differ significantly between the groups, but it did not correlate with any of the PET parameters assessed. Thus, this study does not prove an association between the release of proteases in chronic hepatitis and the permeability of the BBB for ammonia.

Significant backflux of ammonia from brain tissue to blood was shown by Keiding *et al* (2006) and Sørensen *et al* (2009). As far as tracer kinetic modeling of ^{13}N-ammonia PET is concerned, backflux is related to whether or not K_1 is a good approximation of the net clearance K_{met} of ammonia from blood to tissue and therefore can be used for the determination of the ammonia metabolic rate. From the formula of K_{met} within the standard (irreversible) two-tissue compartment model (see 'Tracer kinetic modeling' in 'Patients and methods'), $K_{met} = K_1 * k_3/(k_2 + k_3) = K_1/(1 + k_2/k_3)$, it is easily seen that K_{met} is indeed well approximated by K_1 if the ratio k_2/k_3 is much smaller than 1. In this study, tracer kinetic modeling did not allow reliable estimates of k_2 and k_3. However, the ratio K_{met}/K_1 was significantly smaller than 1 in all groups (Table 1). In the healthy controls the ratio was 0.578 ± 0.134, which is in very good agreement with the results of Sørensen *et al* (Figure 2 in Sørensen *et al*, 2009), and therefore

confirms their finding of significant backflux of ammonia from the brain. From the relation between K_{met} and K_1 given above, one easily finds that the ratio $K_{met}/K_1 = 0.578$ corresponds to $k_2/k_3 = 0.730$, thus not being much smaller than 1. It might be worth noting that the intercept of the Gjedde–Patlak plot was significantly larger than the fbv in all groups (Table 1, global mean *fbv* over all subjects 0.036 ± 0.007). This also indicates significant backflux of ammonia, as the intercept is given by the formula $fbv + K_1^* k_2/(k_2 + k_3)^2$ (Patlak *et al*, 1983).

The magnitude of backflux of ammonia from brain tissue might depend on the blood-to-brain gradient of pH, because of the rather strong pH dependence of the fraction of gaseous ammonia (Lockwood *et al*, 1980). However, a potential effect is expected to be rather small, as the rapid ammonia metabolism in the brain prevents ammonia from reaching equilibrium distribution corresponding to the blood-to-brain pH gradient.

Phelps *et al* (1981) have suggested that differences in regional cerebral ammonia uptake might be largely because of variations in blood flow by both recruitment of capillaries and by variation of blood velocity in open capillaries. In this study, CBF did neither differ globally nor regionally between patients and controls, respectively, between the three patients groups (Table 1). It might be worth noting that the CBF values obtained in this study were systematically lower than those reported in similar patient populations by other groups (Lockwood *et al*, 1991; Ahl *et al*, 2004; Keiding *et al*, 2006; Iversen *et al*, 2006, 2009). Several factors such as differences in age of the subjects, tracer kinetic modeling, degree of liver disease, and definition of VOIs may contribute to this effect. The 'Flow and Dispersion' model used for the kinetic analysis of the ^{15}O-water TACs in this study assumes diffusion equilibrium between tissue and blood. However, ^{15}O-water is a diffusion-limited tracer with a first pass extraction of 0.8 to 0.9. This results in an underestimation of CBF by 10% to 20%. This effect was corrected for in the studies of Keiding *et al* (2006) and Iversen *et al* (2006, 2009) but not in this study. The definition of VOIs has also an impact on the quantification of CBF. In this study, 'large' VOIs were used in predefined template space by the automated anatomic labeling atlas. These VOIs include a rather large fraction of white matter (Figure 2). As CBF in gray matter is three- to four-fold that in white matter (the difference usually being less pronounced in PET scans because of limited spatial resolution), large VOIs result in lower estimates of CBF compared with small VOIs with smaller white matter fraction when the mean voxel intensity over the voxels in the VOI is used to characterize tracer uptake in the VOI (some authors use the maximum voxel intensity). However, large VOIs are less sensitive to residual anatomical variability after stereotactical normalization. We decided to use the automated anatomic labeling atlas, because it is commonly available and thus could be used by other groups. Use of the same VOIs would greatly simplify comparison of the results of different studies.

The estimates of CMRA achieved in the PET studies performed so far differ significantly. In their first study Lockwood *et al* (1984) assessed the CMRA in five healthy subjects as 18 ± 9 nmol/g/min in the gray and 14 ± 8 nmol/g/min in the white matter. In their second study (1991) comparing healthy controls and patients with liver cirrhosis and minimal HE global CMRA was 3.5 ± 1.5 nmol/g/min in controls and 9.1 ± 3.6 nmol/g/min in cirrhotic patients with minimal HE, increasing with arterial ammonia concentrations that differed significantly between both groups. Keiding *et al* (2006) similarly found that CMRA increased with increasing arterial blood concentrations of ammonia, cortex values being 2.6 ± 0.3 nmol/mL/min in healthy controls, 7.4 ± 1.4 nmol/mL/min in cirrhotic patients without HE, and 13.4 ± 0.9 nmol/mL/min in cirrhotic patients with overt HE. In this study, CMRA in healthy controls was 1.9 ± 0.5 nmol/mL/min and thereby especially lower than the value published early by Lockwood *et al* (1984).

The underlying model for both of Lockwood's studies was the irreversible trapping of ammonia and its metabolites in the brain during scan time. Static PET scans were used and measurement was started 10 mins after injection of ^{13}N-ammonia (Lockwood *et al*, 1984). Whether the PS product calculated in these studies is actually PS_{BBB} has been discussed controversially (Lockwood and Wack, 2006). In the healthy subjects of the first study the calculated PS product was 0.32 ± 0.19 mL/g/min in the gray and 0.24 ± 0.16 mL/g/min in the white matter. In the second study, the global PS product in controls was 0.13 ± 0.03 mL/g/min compared with 0.22 ± 0.07 mL/g/min in the patients. Interestingly, the patients' global PS product is comparable to those in this study (Table 1), whereas there are remarkable differences with regard to the data in healthy subjects (PS_{BBB} 0.21 ± 0.05).

Compared with previous studies of cerebral ammonia metabolism in patients with liver disease, the patient groups of this study were quite homogenous. Lockwood *et al* (1991) did not mention the underlying diseases in their patients, Ahl *et al* (2004) included predominantly patients with posthepatitic cirrhosis, but also some with autoimmunologic diseases, and patients of Keiding's study (2006) had mainly alcohol toxic cirrhosis. It is unknown, today, if the different underlying pathologies in the patients might affect the BBB differently, and thus account for the differing results in the studies available at present. It should be emphasized, however, that it is not only a difference in the findings in the patient groups, but the findings in the healthy controls also make up a controversy. The latter most likely is related to methodological issues (Berding *et al*, 2009).

The following limitations of this study should me mentioned.

Radioactive metabolites of ^{13}N-ammonia in blood were not measured during ^{13}N-ammonia PET, but a population-based metabolite correction was used (Ahl *et al*, 2004). This population-based correction was obtained by a monoexponential fit of the data provided by Rosenspire *et al* (1990). These data have been obtained in healthy subjects and therefore use in patients with liver fibrosis might be questionable, as there might be considerable differences in systematic ammonia metabolism depending on the liver status. In fact, Keiding *et al* (2006) recently reported a detailed analysis of the individual metabolite measurements from their study, and found that systemic conversion of ^{13}N-ammonia to ^{13}N-metabolites was significantly slower in cirrhotic patients than in healthy subjects (Keiding *et al*, accepted for publication). However, the effect was most pronounced in cirrhotic patients with HE, whereas the difference between cirrhotic patients without HE and healthy subjects was only small (results of statistical testing were not reported). This suggests that potential alterations in systemic ammonia metabolism in the F2 and F4 patients without significant impairment of liver function included in this study were small. Nevertheless, although the use of the population-based metabolite correction most likely did not cause a systematic bias between the groups of this study, it should be noted that there is considerable interindividual variance in systemic ammonia metabolism even in healthy subjects (Keiding *et al*, accepted for publication). Population-based metabolite correction does not account for this variability, and therefore causes increased variability in the results of tracer kinetic modeling, which in turn reduces the power for detection of differences between groups. However, this mainly affects the net clearance rate K_{met} of ammonia, whereas the rate K_1 of unidirectional transport of ^{13}N-ammonia from blood into tissue is quite stable with respect to the typical variation of systemic ammonia metabolism. This is due to the fact, that K_1 is essentially obtained from the early time points of the dynamic ^{13}N-ammonia PET scan, where the fraction of metabolites is still small. This has been shown recently by Keiding *et al*, who compared K_1 obtained from the irreversible two-tissue compartment model and individually measured metabolite correction with K_1 obtained from the same model but using the blood total activity curve as input function, i.e., without any metabolite correction (Keiding *et al*, accepted for publication). There was no significant difference. The authors concluded that 'it is acceptable to use whole-blood 13N concentrations as input function for assessment of initial brain ammonia kinetics, including estimates of the blood-brain-barrier permeability for ammonia' (Keiding *et al*, accepted for publication). To test this in our own data, the computation of global K_1 was repeated with the total activity curve in blood as input function instead of using the population-based metabolite correction. Then linear regression analysis was performed with global K_1 without metabolite correction as dependent variable and global K_1 with metabolite correction as regressor. The slope was in agreement with 1 (slope = 0.948, $P < 0.0005$, 95% confidence interval 0.894 to 1.002), the constant was in agreement with 0 (constant = 0.004, $P = 0.312$, 95% confidence interval −0.004 to 0.013). Thus, this study confirms the cited conclusion of *K*eiding *et al.* It might be worth noting that this also implies that brain uptake of radioactive metabolites can be neglected as far as the determination of K_1 and BBB permeability for ammonia is concerned.

As K_1, but not K_{met}, is used for the computation of the permeability area surface product PS_{BBB} of the BBB for ammonia, the main result of this study, that there was no significant difference in BBB permeability for ammonia between the healthy controls, F2 and F4 subjects is not affected by any limitation of population-based metabolite correction.

In contrast, the results of the Gjedde–Patlak analysis are affected by the limitation of using a population-based metabolite correction. Both, bias and increased variability cannot be ruled out. The impact of population-based metabolite correction on K_{met} requires further investigation.

The frames in each individual dynamic PET sequence were realigned to correct for eventual head motion during the acquisition. Realignment did not account for the fact that if there are movements between the different frames of a dynamic emission scan, there will also be movements relative to the transmission scan used for attenuation correction. The effects of misalignment between true and assumed attenuating media are well known. For PET studies of the brain, Andersson *et al* (1995), for example, investigated the effect of mismatch between transmission and emission scan. The quantification error caused by mismatch in *x* direction was largest in lateral cortical brain regions, up to 13% for mismatch of 6 mm (from Figure 4 in Andersson *et al*, 1995). However, the quantification error was largely left–right symmetric, i.e., underestimation (overestimation) of tracer uptake in a given VOI in one hemisphere was accompanied by overestimation (underestimation) of tracer uptake in the mirror VOI in the other hemisphere. Therefore, effects on average tracer uptake in two-sided VOIs, i.e., VOIs including both hemispheres, are expected to be rather small. In this study, only two-sided VOIs were used. Nevertheless, the analyses of this study were repeated without the two subjects who had moved more than 6 mm during a PET scan. The results were virtually unchanged. In particular, there were no group differences of global CBF, K_1, PS_{BBB}, K_{met}, or CMRA.

In conclusion, this study provides no evidence for alterations of the permeability of the BBB for ammonia in patients with liver fibrosis compared with healthy controls. It must be admitted, however, that—as for the former studies—the number of patients included is small and thus the results are

worth discussing. At present, we have two studies without any proof of an altered BBB permeability for ammonia in patients with liver disease covering together stages from grades 2 to 6 fibrosis and patients with grades 0 to 4 HE (this study and Keiding *et al*, 2006) compared with one study (Lockwood *et al*, 1991) that indicates a significant increase in the BBB permeability for ammonia in cirrhotic patients compared with controls. Evidence increases that in fact the BBB permeability for ammonia in cirrhotic patients is not altered. However, there are still remaining questions with regard to the most adequate modeling of cerebral ammonia-PET data (Lockwood, 2007), and also doubts if the currently available data represent the whole spectrum of patients with liver fibrosis and cirrhosis. The picture could completely change, for example, in patients with acute decompensation of chronic liver disease, in patients with accompanying severe systemic inflammation, or in patients with acute liver failure. Closing of the chapter with reference to the available data therefore could be premature.

Acknowledgements

We thank Susanne Keiding for providing her most recent paper before publication and her agreement to cite the data. This study was supported by the program, Hochschulinterne Leistungsförderung' (HiLF) of Hannover Medical School.

Conflict of interest

The authors declare no conflict of interest.

References

Ahl B, Weissenborn K, van den Hoff J, Fischer-Wasels D, Köstler H, Hecker H, Burchert W (2004) Regional differences in cerebral blood flow and cerebral ammonia metabolism in patients with cirrhosis. *Hepatology* 40:73–9

Andersson JLR, Vagnhammar BE, Schneider H (1995) Accurate attenuation correction despite movement during PET imaging. *J Nucl Med* 36:670–8

Berding G, Banati RB, Buchert R, Chierichetti F, Grover VPB, Kato A, Keiding S, Taylor-Robinson SD (2009) Radiotracer imaging studies in hepatic encephalopathy: ISHEN practice guidelines. *Liver Int* 29:621–8

Butterworth RF (2003) Pathogenesis of hepatic encephalopathy: new insights from neuroimaging and molecular studies. *J Hepatol* 39:278–85

Carroll TJ, Teneggi V, Jobin M, Squassante L, Treyer V, Hany TF, Burger C, Wang L, Bye A, von Schulthess GK, Buck A (2002) Absolute quantification of cerebral blood flow with magnetic resonance, reproducibility of the method, and comparison with H2(15)O positron emission tomography. *J Cereb Blood Flow Metab* 22:1149–56

Cooper AJL, McDonald JM, Gelbard , Gledhill RF, Duffy TE (1979) The metabolic fate of ^{13}N labeled ammonia in rat brain. *Journal Biol Chem* 254:4982–92

Gjedde A (1982) Calculation of cerebral glucose phosphorylation from brain uptake of glucose analogs *in vivo*: a re-examination. *Brain Res* 257:237–74

Innis RB, Cunningham VJ, Delforge J, Fujita M, Gjedde A, Gunn RN, Holden J, Houle S, Huang SC, Ichise M, Iida H, Ito H, Kimura Y, Koeppe RA, Knudsen GM, Knuuti J, Lammertsma AA, Laruelle M, Logan J, Maguire RP, Mintun MA, Morris ED, Parsey R, Price JC, Slifstein M, Sossi V, Suhara T, Votaw JR, Wong DF, Carson RE (2007) Consensus nomenclature for *in vivo* imaging of reversibly binding radioligands. *J Cereb Blood Flow Metab* 27:1533–9

Iversen P, Hansen DA, Bender D, Rodell A, Munk OL, Cumming P, Keiding S (2006) Peripheral benzodiazepine receptors in the brain of cirrhosis patients with manifest hepatic encephalopathy. *Eur J Nucl Med Mol Imaging* 33:810–6

Iversen P, Sørensen M, Bak LK, Waagepetersen HS, Vafaee MS, Borghammer P, Mouridsen K, Jensen SB, Vilstrup H, Schousboe A, Ott P, Gjedde A, Keiding S (2009) Low cerebral oxygen consumption and blood flow in patients with cirrhosis and an acute episode of hepatic encephalopathy. *Gastroenterology* 136:863–71

Keiding S, Sørensen M, Bender D, Lajord Munk O, Ott P, Vilstrup H (2006) Brain metabolism of ^{13}N-ammonia during acute hepatic encephalopathy in cirrhosis measured by positron emission tomography. *Hepatology* 43:42–50. Erratum (2006) Hepatology 44:1056

Keiding S, Sørensen M, Munk OL, Bender D. Human 13N-ammonia PET studies: The importance of measuring 13N-ammonia metabolites in blood. *Metab Brain Dis*, accepted for publication

Köstler H (1998) Proton magnetic resonance spectroscopy in portal-systemic encephalopathy. *Metab Brain Dis* 13:291–301

Lockwood AH, Finn RD, Campbell JA, Richman TB (1980) Factors thataffect the uptake of ammonia by the brain: The blood-brain ph Gradient. *Brain Res* 181: 259–266

Lockwood AH, Bolomey L, Napoleon F (1984) Blood-brain barrier to ammonia in humans. *J Cereb Blood Flow Metab* 4:516–22

Lockwood AH, Yap EWH, Wong W-H (1991) Cerebral ammonia metabolism in patients with severe liver disease and minimal hepatic encephalopathy. *J Cereb Blood Flow Metab* 11:337–41

Lockwood AH, Wack DS (2006) The brain permeability-surface product for ammonia. *Hepatology* 44:1052–3; author reply 1053–1054

Lockwood AH (2007) Controversies in ammonia metabolism: implications for hepatic encephalopathy. *Metab Brain Dis* 22:285–9

Patlak CS, Blasberg RG, Fenstermacher JD (1983) Graphical evaluation of blood-to-brain transfer constants from multiple- time uptake data. *J Cereb Blood Flow Metab* 3:1–7

Phelps ME, Hoffman EJ, Raybaud C (1977) Factors whichaffect cerebral uptake and retention of $^{13}NH_3$. *Stroke* 8:694–702

Phelps ME, Huang S-C, Hoffman EJ, Selin C, Kuhl DE (1981) Cerebral extraction of N-13 ammonia: Its dependence on cerebral blood flow and capillary permeability-surface area product. *Stroke* 12:607–19

Pugh RNH, Murray-Lyon IM, Dawson JL, Pietroni MC, Will R (1973) Transection of the oesophagus for bleeding oesophageal varices. *Br J Surg* 60:646–9

Rosenspire KC, Schwaiger M, Mangner TJ, Hutchins GD, Sutorik A, Kuhl DE (1990) Metabolic fate of [13N]ammonia in human and canine blood. *J Nucl Med* 31:163–7

Schomerus H, Weissenborn K, Hamster W, Rueckert N, Hecker H (1999) *PSE-Syndrom-Test. Psychodiagnostisches Verfahren zur quantitativen Erfassung der (minimalen) portosystemischen Enzephalopathie*. Frankfurt: Swets Test Services

Sørensen M, Munk OL, Keiding S (2009) Backflux of ammonia from brain to blood in human subjects with and without hepatic encephalopathy. *Metab Brain Dis* 24:237–42

Tzourio-Mazoyer N, Landeau B, Papathanassiou D, Crivello F, Etard O, Delcroix N, Mazoyer B, Joliot M (2002) Automated anatomical labeling of activations in SPM using a macroscopic anatomical parcellation of the MNI MRI single-subject brain. *Neuroimage* 15:273–89

van den Hoff J, Burchert W, Börner AR, Fricke H, Kühnel G, Meyer GJ, Otto D, Weckesser E, Wolpers HG, Knapp WH (2001) [1-(11)C]Acetate asa quantitative perfusion tracer in myocardial PET. *J Nucl Med* 42:1174–82

van den Hoff J, Burchert W, Müller-Schauenburg W, Meyer GJ, Hundeshagen H (1993) Accurate local blood flow measurements with dynamic PET: fast determination of input function delay and dispersion by multilinear minimization. *J Nucl Med* 34:1770–7

Weissenborn K, Ahl B, Fischer-Wasels D, van den Hoff J, Hecker H, Burchert W, Köstler H (2007) Correlations between MRS alterations and cerebral ammonia and glucose metabolism in cirrhotic patients with and without hepatic encephalopathy. *GUT* 56:1736–42